

Super-Droplet Kernels - backend-level routines for Monte-Carlo particle coagulation solvers: API proposal with CPU and GPU implementation in Python ^{*}

Piotr Bartman¹[0000-0003-0265-6428] and Sylwester Arabas¹[0000-0003-2361-0082]

Jagiellonian University, Kraków, Poland

`piotr.bartman@doctoral.uj.edu.pl`, `sylwester.arabas@uj.edu.pl`

Abstract. Super-Droplet Method (SDM) is a probabilistic Monte-Carlo-type model of particle coagulation process, an alternative to the mean-field formulation of Smoluchowski. SDM as an algorithm has linear computational complexity with respect to the state vector length, the state vector length is constant throughout simulation, and most of the algorithm steps are readily parallelisable. This paper discusses the design and implementation of two number-crunching backends for SDM implemented in PySDM, a new free and open-source Python package for simulating the dynamics of atmospheric aerosol, cloud and rain particles (<https://github.com/atmos-cloud-sim-uj/PySDM>). The two backends share their application programming interface (API) but leverage distinct parallelism paradigms, target different hardware, and are built on top of different lower-level routine sets. First offers multi-threaded CPU computations and is based on Numba (using Numpy arrays). Second offers GPU computations and is built on top of ThrustRTC and CURandRTC (and does not use Numpy arrays). The paper puts forward a proposal of the Super-Droplet Kernels API featuring data structures and backend-level routines (computational kernels) suitable for performing the computational steps SDM consists of. Presented discussion covers: data dependencies across steps, parallelisation opportunities, CPU and GPU implementation nuances, and algorithm workflow. Example simulations suitable for validating implementations of the API are presented.

Keywords: Monte-Carlo · coagulation · Super-Droplet Method · GPU.

1 Introduction

The Super-Droplet Method (SDM) introduced in [18] is a computationally efficient Monte-Carlo type algorithm for modelling the process of collisional growth (coagulation) of particles. SDM was introduced in the context of atmospheric modelling, in particular for simulating the formation of cloud and rain (hence

^{*} Funding: Foundation for Polish Science (POIR.04.04.00-00-5E1C/18-00).

the algorithm name) through particle-based simulations. Such simulations couple a grid-based computational fluid-dynamics (CFD) core with a probabilistic, so-called super-particle (hence the algorithm name), representation of the particulate phase, and constitute a unique tool for comprehensive modelling of aerosol-cloud interactions (see, e.g., [3,13]). The probabilistic character of SDM is embodied, among other aspects, in the assumption of each super-particle representing a multiple number of modelled droplets with the same attributes (including particle size and position in space). The super-droplets are thus a coarse-grained view of droplets both in physical space and attribute space.

The probabilistic description of collisional growth has a wide range of applications across different domains of computational sciences (e.g., astrophysics, aerosol/hydrosol technology including combustion). While focused on SDM and depicted with atmospheric phenomena examples, the material presented herein is generally applicable in development of software implementing other Monte-Carlo type schemes for coagulation (e.g., Weighted Flow Algorithms [8] and other, see Sect. 1 in [19]), particularly when sharing the concept of super-particles.

The original algorithm description [18], the relevant patent applications (e.g., [20]) and several subsequent works scrutinising SDM (e.g., [2,17,9,23]) expounded upon the algorithm characteristics from users' (physicists') point of view. The aim of this work is to discuss the algorithm from software developer's perspective. To this end, the scope of the discussion covers: data dependencies, parallelisation opportunities, state vector structure and helper variable requirements, minimal set of computational kernels needed to be implemented and the overall algorithm workflow. Throughout the paper, these concepts are depicted with pseudo-code-mimicking Python snippets (syntactically correct and runnable), but the solutions introduced are not bound to a particular language. In contrast, the gist of the paper is the language-agnostic API (i.e., application programming interface) proposal put forward with the very aim of capturing the implementation-relevant nuances of the algorithm which are, arguably, tricky to discern from existing literature on SDM, yet which have profound impact on the simulation performance. The API provides an indirection layer separating higher-level physically-relevant concepts from lower-level computational kernels.

Validity of the proposed API design has been demonstrated with two distinct backend implementations included in a newly developed simulation package PySDM [5]. The two backends share the programming interface, while differing substantially in the underlying software components and the targeted hardware (CPU vs. GPU). PySDM is free and open source software, presented results are readily reproducible with examples included in the v1.1 release of PySDM.

The remainder of this paper is structured as follows. Section 2 briefly introduces the SDM algorithm through a juxtaposition against the alternative classic Smoluchowski's coagulation equation (SCE). Section 3 defines the proposed backend API. Section 4 presents simulations performed with the PySDM package based on benchmark setups from literature and used to depict the algorithm scalability and CPU vs. GPU performance. Section 5 concludes the work enumerating the key points brought out in the paper.

2 SDM as compared to SCE

2.1 Mean-field approach: Smoluchowski's coagulation equation

Population balance equation which describes collisional growth is historically known as the Smoluchowski's coagulation equation (SCE) and was introduced in [22,21] (for a classic and recent overviews, see e.g. [7] and [14], respectively). Noteworthy, it is formulated under the mean-field assumptions of sufficiently large system and of neglected correlations between numbers of droplets of different sizes (for discussion, see [9]).

Let function $c(x, t) : \mathbb{R}^+ \times \mathbb{R}^+ \rightarrow \mathbb{R}^+$ correspond to particle size spectrum and describe the average concentration of particles of size x at time t in a well-mixed volume of air V . Smoluchowski's coagulation equation describes evolution of particle size spectrum in time due to collisions. For convenience, t is skipped in notation: $c(x) = c(x, t)$, while \dot{c} denotes partial derivative with respect to time.

$$\dot{c}(x) = \frac{1}{2} \int_0^x a(y, x-y)c(y)c(x-y)dy - \int_0^\infty a(y, x)c(y)c(x)dy \quad (1)$$

where $a(x_1, x_2)$ is the so-called kernel which defines the rate of collisions (and coagulation) between particles of sizes x_1 and x_2 and $a(x_1, x_2) = a(x_2, x_1)$. The first term on the right-hand side is the production of particles of size x by coalescence of two smaller particles and the factor $1/2$ is for avoiding double counting. The second term represents the reduction in number of colliding particles due to coagulation.

The Smoluchowski's equation has an alternative form that is discrete in size space. Let x_0 be the smallest considered difference of size between particles, $x_i = ix_0$, $i \in \mathbb{N}$ and $c_i = c(x_i)$ then:

$$\dot{c}_i = \frac{1}{2} \sum_{k=1}^{i-1} a(x_k, x_{i-k})c_k c_{i-k} - \sum_{k=1}^{\infty} a(x_k, x_i)c_k c_i \quad (2)$$

Analytic solutions to the equation are known only for simple kernels ([14]), such as: constant $a(x_1, x_2) = 1$, additive $a(x_1, x_2) = x_1 + x_2$ (Golovin's kernel) or multiplicative $a(x_1, x_2) = x_1 x_2$. Taking atmospheric physics as an example, collisions of droplet within cloud occur by differentiated movements of particles caused by combination of gravitational, electrical, or aerodynamic forces, where gravitational effects dominate. As such, sophisticated kernels are needed to describe these phenomena, and hence numerical methods are required for solving the coagulation problem. However, when multiple properties of particles (such as volume, temperature, concentration of chemical compounds, etc.) need to be taken into account, the numerical methods for SCE suffer from the curse of dimensionality due to the need to distinguish particles of same size x but different properties.

Additionally, it is worth to highlight that, in practice, the assumptions of the Smoluchowski equation may be difficult to meet. First, the particle size changes

at the same time due to processes other than coalescence (condensation/evaporation). Second, it is assumed that the system is large enough and the droplets inside are uniformly distributed, which in turn is only true for a small volume in the atmosphere. Moreover, using the Smoluchowski's equation that describes evolution of the mean state of the system, leads to deterministic simulations. The alternative to Smoluchowski equation are Monte-Carlo methods based on stochastic model of the collision-coalescence process. Embracing stochastic approach enables simulating ensembles of realisations of the process aiding studies of rare (far-from-the-mean) phenomena like rapid precipitation onset (see discussion in [13]).

Despite the above limitations, the Smoluchowski's equation and the analytical solutions of SCE are important for validation of alternative methods and are used for this purpose herein.

2.2 Monte-Carlo approach: Super-Droplet Method (SDM)

All mentioned problems related to Smoluchowski's equation were the reasons to look for alternative methods. The stochastic coalescence model for cloud droplet growth was already analysed by Gillespie in [11]. There were however still challenges (described below) related to computational and memory complexity which were solved and applied by Shima et al. in [18] (and extended to cover clouds featuring ice phase of water in [19]). The Monte-Carlo numerical scheme introduced in [18] is referred to as the Super-Droplet Method (SDM).

Tracking all particles in large simulations has immeasurably high computational cost, which is why the notion of super-particles is introduced, but still in many cases it can be treated in the same way as real particles. For convenience, let Ξ_{part} and Ξ_{sd} be indexed sets of real-droplets and super-droplets, respectively. Each element of these sets has unique index $i \in [0, 1, \dots, n_{part} - 1]$ (or $i \in [0, 1, \dots, n_{sd} - 1]$), where (n_{sd}) n_{part} is a number of considered (super) droplets. Attributes related to a specific (super) droplet i are denoted by $attr_{[i]}$. Example droplet attributes are: position, volume v of droplet, volume of substances dissolved in particle.

In the probabilistic particle-based approach, each super-droplet represents a multiple number of droplets with the same attributes (including position) and is assigned with a *multiplicity* value denoted by $\xi \in \mathbb{N}$ and which can be different in each super-droplet. In SDM, multiplicity $\xi_{[i]}$ of super-droplet of size $x_{[i]}$ is conceptually related to $c_i = c(x_i)$ from equation (2).

The number of super-droplets must be sufficient to cover the phase space of particle properties, and the higher the number, the smaller the multiplicities and the higher fidelity of discretisation (see discussion in [18,19]).

The algorithm steps, as defined in [18], can be outlined as follows and table 1 summarises the main differences between the SCE and SDM:

Step 1: cell-wise shuffling

In SCE, all considered droplets are compared with each other and a fraction of droplets of size $x_{[i]}$ collides with a fraction droplets of size $x_{[j]}$ in each time step.

In contrast, in SDM a random set of $\lfloor n_{sd}/2 \rfloor$ non-overlapping pairs is considered in each time step, where n_{sd} is the number of super-droplets.

To ensure linear computational complexity, the mechanism for choosing random non-overlapping pairs must also have at most linear computational complexity. It can be obtained by permuting an indexed array of super-droplets where each pair consist of super-droplets with indexes $(2j)$ and $(2j + 1)$ where $j \in [0, 1, 2, \dots, n_{sd})$ (see appendix A in [18]).

Step 2: collision probability evaluation

If a fraction of droplets is allowed to collide, a collision of two super-droplets can produce third super-droplet which has different size. To represent such collision event, a new super-droplet would need to be added to the system what leads to: increasing the number of super-droplets in the system, smaller and smaller multiplicities and increasing memory demands during simulation. Moreover, it is hard to predict at the beginning of a simulation how much memory is needed (see discussion in [15]). Adding new super-droplets can be avoided by mapping colliding super-droplets to a multi-dimensional grid (e.g., 2D for particle volume and its dry size), simulating coalescence on this grid using SCE-based approach and discretising the results back into Lagrangian particles as proposed in [1]. Such approach however, not only entails additional computational cost, but most importantly is characterised by the very curse of dimensionality and numerical diffusion that were meant to be avoided by using particle-based technique.

SDM avoids the issue of unpredictable memory complexity stemming from the need of allocating space for freshly collided super-particle of size that differs from the size of the colliding ones. To this end, in SDM only collisions of all of $\min\{\xi_{[i]}, \xi_{[j]}\}$ droplets are considered, and thus collision of two super-droplets always produces 1 or 2 super-droplets. This means there is no need for adding extra super-droplets to the system during simulation.

For each pair, probability of collision p is determined by up-scaled to number of real droplets represented by the super-droplet with higher multiplicity ($\max\{\xi_{[i]}, \xi_{[j]}\}$). As a result, computational complexity is $\mathcal{O}(n_{sd})$ instead of $\mathcal{O}(n_{sd}^2)$ what is a significant gain.

The evaluated probability of collision of super-droplets requires further up-scaling due to the reduced amount of sampled candidate pairs as outlined in Step 1 above. To this end, the probability is multiplied by the ratio of the number of all non-overlapping pairs $(n_{sd}^2 - n_{sd})/2$ to the number of considered candidate pairs $\lfloor n_{sd}/2 \rfloor$.

For each selected pair of j -th and k -th super-droplets, the probability p of collision of the super-droplets within time interval Δt is thus evaluated as:

$$p = a(v_{[j]}, v_{[k]}) \max\{\xi_{[j]}, \xi_{[k]}\} \frac{(n_{sd}^2 - n_{sd})/2}{\lfloor n_{sd}/2 \rfloor} \frac{\Delta t}{\Delta V} \quad (3)$$

where a is a coalescence kernel (e.g. based on collision cross-section geometry) and ΔV is the considered volume (of air) assumed to be mixed well enough to neglect the positions of particles when evaluating the probability of collision.

Table 1. Comparison of SCE and SDM approaches to modelling collisional growth.

	SCE (mean-field)	SDM (probabilistic)
considered pairs	all (i,j) pairs	random set of $n_{sd}/2$ non-overlapping pairs,
comp. complexity	$\mathcal{O}(n_{sd}^2)$	probability up-scaled by $(n_{sd}^2 - n_{sd})/2$ to $n_{sd}/2$ ratio
collisions	colliding a fraction of $\xi_{[i]}, \xi_{[j]}$	$\mathcal{O}(n_{sd})$
collisions triggered	every time step	collide all of $\min\{\xi_{[i]}, \xi_{[j]}\}$ (all or nothing) by comparing probability with a random number

Step 3: collision triggering and attribute updates

In the spirit of Monte-Carlo methods, the collisions are triggered with a random number $\phi_\gamma \sim Uniform[0, 1)$, and the rate of collisions γ (per timestep) is:

$$\gamma = \lceil p - \phi_\gamma \rceil \quad (4)$$

with $\gamma \in \mathbb{N}$. Noting that the rate γ can be greater than 1, a further adjustment is introduced with the aim of representing multiple collision of super-particles:

$$\tilde{\gamma} = \min\{\gamma, \lfloor \xi_{[j]}/\xi_{[k]} \rfloor\} \quad (5)$$

where $\xi_{[j]} > \xi_{[k]}$ was assumed (without losing generality).

Coalescence of two droplets results in creation of a new droplet with new attributes. Two kinds of attributes are distinguished: extensive $A^{ex} \in \mathbb{R}^{n_{ex}}$ and intensive $A^{in} \in \mathbb{R}^{n_{in}}$, and n_{ex}, n_{in} are the numbers of extensive and intensive attributes, respectively. During coalescence, values of extensive attributes of collided droplets add up. In the intensive case, the result is a volume-weighted average of pre-collision values. Examples of extensive attributes are: volume, dry volume or heat content; examples of intensive attributes are: temperature or concentration of chemical compounds. Values of attributes of super-droplets after collision are denoted by hat. There are two cases:

1. $\xi_{[j]} - \tilde{\gamma}\xi_{[k]} > 0$

$$\begin{aligned} \hat{\xi}_{[j]} &= \xi_{[j]} - \tilde{\gamma}\xi_{[k]} & \hat{\xi}_{[k]} &= \xi_{[k]} \\ \hat{A}_{[j]}^{ex} &= A_{[j]}^{ex} & \hat{A}_{[k]}^{ex} &= A_{[k]}^{ex} + \tilde{\gamma}A_{[j]}^{ex} \\ \hat{A}_{[j]}^{in} &= A_{[j]}^{in} & \hat{A}_{[k]}^{in} &= \frac{A_{[k]}^{in}v_{[k]} + \tilde{\gamma}A_{[j]}^{in}v_{[j]}}{v_{[k]} + \tilde{\gamma}v_{[j]}} \end{aligned} \quad (6)$$

2. $\xi_{[j]} - \tilde{\gamma}\xi_{[k]} = 0$

$$\begin{aligned} \hat{\xi}_{[j]} &= \lfloor \xi_{[k]}/2 \rfloor & \hat{\xi}_{[k]} &= \xi_{[k]} - \lfloor \xi_{[k]}/2 \rfloor \\ \hat{A}_{[j]}^{ex} &= \hat{A}_{[k]}^{ex} & \hat{A}_{[k]}^{ex} &= A_{[k]}^{ex} + \tilde{\gamma}A_{[j]}^{ex} \\ \hat{A}_{[j]}^{in} &= \hat{A}_{[k]}^{in} & \hat{A}_{[k]}^{in} &= \frac{A_{[k]}^{in}v_{[k]} + \tilde{\gamma}A_{[j]}^{in}v_{[j]}}{v_{[k]} + \tilde{\gamma}v_{[j]}} \end{aligned} \quad (7)$$

If in eq. (7) multiplicity $\hat{\xi}_{[j]} = 0$, the j -th super-droplet is removed from the system (happens only if, as a result of a collision, one single real droplet is created). The conceptual view of collision of two super-droplets is intuitively depicted in Fig.1 in [18].

3 Super-Droplet Kernels API

The proposed API is composed of four data structures (classes) and 9 library routines (involving computational kernels). Description below outlines both the general, implementation-independent, structure of the API, as well as selected aspects pertaining to the experience from implementing CPU and GPU backends in the PySDM package. These were built on top of the Numba [16] and ThrustRTC [25] Python packages, respectively. Numba is a just-in-time (JIT) compiler for Python code, it features extensive support for Numpy constructs and features multi-threading constructs akin to the OpenMP infrastructure. ThrustRTC uses the NVIDIA CUDA real-time compilation infrastructure offering high-level Python interface for execution of both built-in and custom computational kernels on GPU.

In multi-dimensional simulations coupled with a grid-based CFD fluid flow solver, the positions of droplets within the physical space are used to split the super-particle population among grid cells (CFD solver mesh). Since positions of droplets change based on the fluid flow and droplet mass/shape characteristics, the particle-cell mapping changes throughout the simulation. Collisions are considered only among particles belonging to the same grid cell, and the varying number of particles within a cell is needed to be tracked at each timestep to evaluate the super-particle collision rates. Figure 1 outlines the setting.

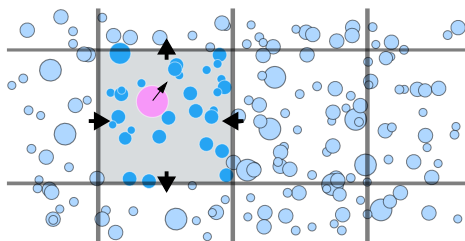


Fig. 1. Schematic of how a CFD grid is populated with immersed super-particles.

3.1 Data structures and simulation state

The **Storage** class is a base container which is intended to adapt the interfaces of the underlying implementation-dependent array containers (in PySDM: Numpy or ThrustRTC containers for CPU and GPU backends, respectively). This removes the dependency of the underlying storage layer in the code utilising the Super-Droplet Kernels API.

The **Storage** class has 3 attributes: data (in PySDM: an instance of Numpy `ndarray` or an instance of ThrustRTC `DVVector`), shape (which specifies size and dimension) and dtype (data type: `float` or `int`). The proposed API employs one- and two-dimensional arrays, implementations of the **Storage** class feature an indirection layer handling the multi-dimensionality in case the underlying library supports one-dimensional indexing only (as in ThrustRTC).

```

1 idx = Index(N_SD, int)
2 multiplicities = IndexedStorage(idx, N_SD, int)
3 intensive = IndexedStorage(idx, (N_IA, N_SD), float)
4 extensive = IndexedStorage(idx, (N_EA, N_SD), float)
5 volume_view = extensive[0:1, :]
6
7 cell_id = IndexedStorage(idx, N_SD, int)
8 cell_idx = Index(N_CELL, int)
9 cell_start = Storage(N_CELL + 1, int)
10
11 pair_prob = Storage(N_SD//2, float)
12 pair_flag = PairIndicator(N_SD, bool)
13
14 u01 = Storage(N_SD, float)

```

Fig. 2. Simulation state example with N_SD super-particles, N_CELL grid cells, N_IA intensive and N_EA extensive attributes.

Storage handles memory allocation and optionally the host-device (CPU-accessible and GPU-accessible memory) data transfers. Equipping **Storage** with an override of the `[]` operator as done in PySDM can be helpful for debugging and unit testing (in Python, **Storage** instances may then be directly used with `max()`, `min()`, etc.), care needs to be taken to ensure memory-view semantics for non-debug usage, though. Explicit allocation is used only (once per simulation),

The **IndexedStorage** subclass of **Storage** is intended as container for super-particle attributes. In SDM, at each step of simulation a different order of particles needs to be considered. To avoid repeated permutations of the attribute values, the **Index** subclass of **Storage** is introduced. One instance of **Index** is shared between **IndexedStorage** instances and is referenced by the `idx` field.

The **Index** class features permutation and array shrinking logic (allowing for removal of super-droplets from the system). To generate permutation of particles, it is enough to permute **Index** only. To handle multi-dimensional simulations, **Index** features sort-by-key logic where a cell id attribute is used as the key.

The **PairIndicator** class provides an abstraction layer facilitating pairwise operations inherent to several steps of the SDM workflow. In principle, it represents a Boolean flag per each super-particle indicating whether in the current state (affected by random shuffling and physical displacement of particles), a given particle is considered as first-in-a-pair. Updating **PairIndicator**, it must be ensured that the next particle according to a given **Index** is the second one in a pair – i.e., resides in the same grid cell. The **PairIndicator** is also used to seamlessly handle odd and even counts of super-particles within a cell.

Figure 2 lists a minimal set of instances of the data structures constituting an SDM-based simulation state and elaborated on in the following section.

3.2 Algorithm workflow and API routines

The algorithm workflow, encoded in Python using the proposed data structures, and divided into the same algorithm steps as outlined in Sec. 2 is given in Fig. 3. An additional Step 0 is introduced to account for handling the removal of zero-multiplicity super-particles at the beginning of each timestep.

The `cell_id` attribute represents particle-cell mapping. Furthermore, the `cell_idx` helper `Index` instance can be used to specify the order in which grid cells are traversed – for parallel execution scheduling purposes. Both `cell_id` and `cell_idx` are updated before entering into the presented block of code.

Step 1 logic begins with generation of random numbers used for random permutation of the particles (in PySDM, CURandRTC [24] is used for parallel execution). It serves as a mechanism for random selection of super-particle pairs in each grid cell. First, a shuffle-per-cell step is done in which the `cell_start` array is updated to indicate the location within cell-sorted `idx` where sets of super-particles belonging to a given grid cell start. Second, the `pair_flag` indicator is updated using the particle-cell mapping embodied in `cell_start`.

It is worth noting that the shuffle-per-cell operation can be implemented using either (i) a domain-global permutation followed by a global sort-by-cell (used for GPU in PySDM) or (ii) a cell-local permutation in which case the global sort-by-cell operation is done beforehand (used for CPU in PySDM). The strategy depends on the computational complexity of the employed permutation and sorting algorithms (solutions such as MergeShuffle [4] are to be tested). For the sort-by-cell operation, PySDM features a parallel counting sort with linear complexity.

Instructions in Step 2 and Step 3 blocks correspond to the evaluation of subsequent terms of equation 3 and the collision event handling. To exemplify the way the GPU and CPU backends are engineered in PySDM, the implementation of the times-max routine with ThrustRTC, and the update-attributes routine with Numba, respectively, are given in Fig. 4.

```

1 # step 0: removal of super-droplets with zero multiplicity
2 remove_if_equal_0(idx, # in/out
3 multiplicities) # in
4
5 # step 1: cell-wise shuffling, pair flagging
6 urand(u01)
7 shuffle_per_cell(cell_start, # out
8 idx, # in/out
9 cell_idx, cell_id, u01) # in
10
11 flag_pairs(pair_flag, # out
12 cell_id, cell_idx, cell_start) # in
13
14 # step 2: collision probability evaluation
15 coalescence_kernel(pair_prob, # out
16 pair_flag, volume_view) # in
17
18 times_max(pair_prob, # in/out
19 multiplicities, pair_flag) # in
20
21 normalize(pair_prob, # in/out
22 dt, dv, cell_id, cell_idx, cell_start) # in
23
24 # step 3: collision triggering and attribute updates
25 urand(u01[:N_SD//2])
26 compute_gamma(pair_prob, # in/out
27 u01[:N_SD//2]) # in
28
29 update_attributes(multiplicities, intensive, extensive, # in/out
30 volume_view, pair_prob) # in

```

Fig. 3. Algorithm workflow within a timestep, in/out comments mark argument intent.

```

1 _kernel = ThrustRTC.For(['data_out', 'perm_in', 'pair_flag'], "i", '''
2     if (pair_flag[i])
3         data_out[i/2] *= max(perm_in[i], perm_in[i + 1]);
4     ''')
5
6 def _launch(length, data_out, data_in, pair_flag, idx):
7     perm_in = trtc.DVPermutation(data_in, idx)
8     _kernel.launch_n(length, [data_out, perm_in, pair_flag])
9
10 def times_max(this, other, pair_flag):
11     _launch(len(other.idx),
12            this.data,                                # in/out
13            other.data, pair_flag.indicator.data, other.idx.data) # in

1 @numba.njit(parallel=True, error_model='numpy')
2 def _update_attributes(length, n, intensive, extensive, volume, idx, gamma):
3     for i in prange(length//2):
4         j = idx[2*i]
5         k = idx[2*i + 1]
6         if n[j] < n[k]:
7             j, k = k, j
8         g = min(int(gamma[i]), int(n[j] / n[k]))
9         if g == 0:
10            continue
11         new_n = n[j] - g * n[k]
12         if new_n > 0:
13             n[j] = new_n
14             for attr in range(0, len(intensive)):
15                 intensive[attr, k] = (intensive[attr, k] * volume[k] +
16                                     intensive[attr, j] * volume[j] * g
17                                     ) / (volume[k] + g * volume[j])
18             for attr in range(0, len(extensive)):
19                 extensive[attr, k] += g * extensive[attr, j]
20         else: # new_n == 0
21             n[j] = n[k] // 2
22             n[k] = n[k] - n[j]
23             for attr in range(0, len(intensive)):
24                 intensive[attr, j] = (intensive[attr, k] * volume[k] +
25                                     intensive[attr, j] * volume[j] * g
26                                     ) / (volume[k] + g * volume[j])
27                 intensive[attr, k] = intensive[attr, j]
28             for attr in range(0, len(extensive)):
29                 extensive[attr, j] = extensive[attr, j] * g \
30                     + extensive[attr, k]
31                 extensive[attr, k] = extensive[attr, j]
32
33 def update_attributes(n, intensive, extensive, volume, gamma):
34     _update_attributes(len(n.idx),
35                       n.data, intensive.data, extensive.data, # in/out
36                       volume.data, n.idx.data, gamma.data) # in

```

Fig. 4. GPU (top panel) and CPU (bottom panel) routine implementation examples.

4 Example simulations

This section outlines a set of test cases useful in validating implementation of the proposed API. First, a simulation constructed analogously as that reported in Fig. 2 in the original SDM paper [18] is proposed. The aim is to corroborate results obtained with SDM against Golovin’s [12] analytical solution to the Smoluchowski’s equation for an additive $a(x_1, x_2) = x_1 + x_2$ coalescence kernel. Results obtained with PySDM are presented in Figure 5.

Figure 6 documents simulation wall times for the above test case measured as a function of number of super-particles employed. Wall times for CPU (Numba) and GPU (ThrustRTC) backends are compared depicting a five-fold GPU-to-CPU speedup for large state vectors (tested on commodity hardware: Intel Core i7-10750H CPU and NVIDIA GeForce RTX 2070 Super Max-Q GPU). Furthermore, the expected asymptotic linear scaling is hinted.

Figure 7 exemplifies simulation with a more realistic coalescence kernels (see figure caption). Since the analytic solution is not known in such case, the results are juxtaposed with figures reproduced from a classic paper on the subject [6].

In all plots, results of the SDM are plotted by aggregating super-particle multiplicities onto a grid of ca. 100 bins, and smoothing the result twice with a running average with a centred five-bin window.

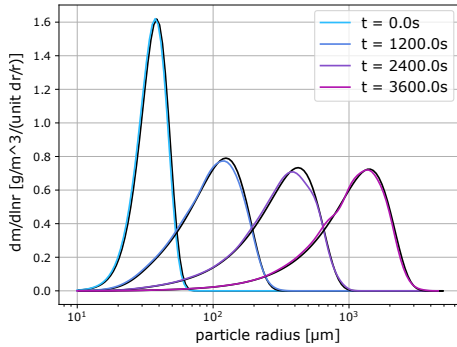


Fig. 5. Particle mass spectrum: SDM results (colour) vs. analytic solution (black).

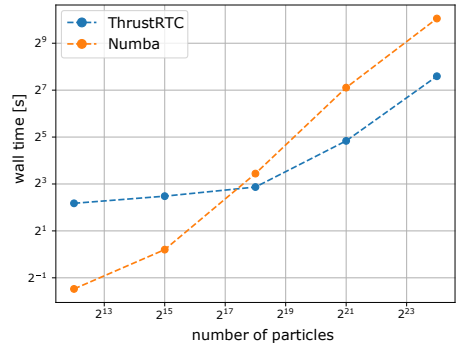


Fig. 6. Simulation wall time as a function of state vector size.

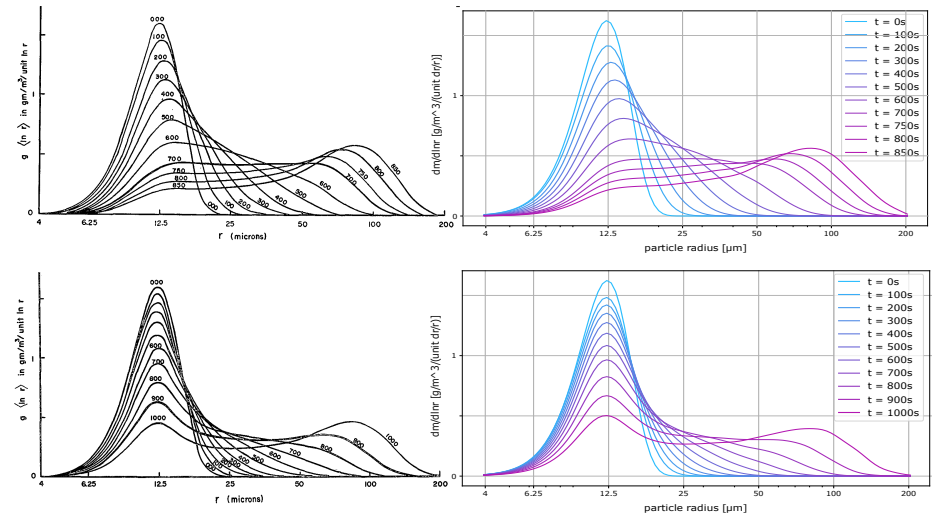


Fig. 7. Left panels show Figs. 5 and 8 from [6]. Right panels depict solutions obtained with PySDM. Top: gravitational kernel; bottom: kernel modelling electric field effect.

5 Summary and discussion

This paper has introduced the **Super-Droplet Kernels API** – a set of **data structures and computational kernels** constituting a number-crunching backend API for the Super-Droplet Method Monte-Carlo algorithm for representing **collisional growth of particles (coagulation)**. Employment of the API assures separation of concerns, in particular separation of parallelisation logic embedded in the backend-level routines from domain logic pertinent to the algorithm workflow. This improves code readability, paves the way for modular design and testability, which all contribute to maintainability of the code base.

The presented SDM algorithm and API descriptions discern data dependencies across the steps of the algorithm (including in/out parameter “intent”) and highlight parallelisation opportunities in different steps. Most of the discerned steps of the SDM algorithm are characterised by some degree of freedom in terms of their implementation. Embracing the API shall help in introducing a dependency injection mechanism allowing unit testing of selected steps and profiling performance with different variants of implementation.

The design of the API has been proved, in the sense of reused abstraction principle, within the **PySDM project** [5] where two backends sharing the API offer contrasting implementations **for CPU and GPU computations**. Both backends are implemented in Python, however: (i) they are targeting different hardware (CPU vs. GPU), (ii) they are based on different underlying technology (Numba: LLVM-based JIT compiler, and ThrustRTC: NVRTC-based runtime compilation mechanism for CUDA), and (iii) they even do not share the de-facto-standard Python Numpy arrays as the storage layer. This highlights that the introduced API is not bound to particular implementation choices, and in particular its **design is applicable to other languages than Python**. At the same time, the case of PySDM is an apt example of how the Python language can be used for high performance computational modelling without trading off the **salient features of Python**:

- succinct syntax** – the pseudo-code snippets presented in the paper are actually valid Python code;
- seamless portability** depicted in PySDM with continuous integration workflows for Linux, macOS and Windows, including 32-bit and 64-bit runs;
- unmatched interoperability** depicted in PySDM with Matlab and Julia usage examples which do not require any additional biding logic within PySDM;
- multifaceted ecosystem** including vibrant market of cloud-computing solutions and depicted in PySDM with one-click execution of Jupyter notebooks on mybinder.org and colab.research.google.com platforms;
- availability of tools for modern hybrid hardware** depicted in PySDM with the GPU backend.

It is worth noting that the above features play well together. For instance, the GPU backend of PySDM featuring the pseudo-code-like API can be leveraged through Jupyter notebooks in the cloud, as well as from within Matlab code on different operating systems.

Bringing the discussion back to the characteristics of the SDM algorithm, it is worth pointing out that, in the **super-particle CFD-coupled simulations** context SDM was introduced and gained attention in, the scheme is particularly **well suited for leveraging modern hybrid CPU-GPU hardware**. First, the algorithm is (almost) embarrassingly parallel. Second, the CPU-GPU transfer overhead is not a bottleneck when GPU-resident dispersed phase representation (super-particles) is coupled with CPU-computed CFD for the continuous phase (fluid flow) as only statistical moments of the size spectrum of the particles is needed for the CFD coupling (see [2]). Third, the CPU and GPU resources on hybrid hardware can be leveraged effectively as the CFD and super-particles components of the simulation system can run simultaneously (see [10]).

Overall, the proposed API prioritises simplicity and was intentionally presented in a paradigm-agnostic pseudo-code-mimicking way, leaving such aspects as object orientation up to the implementation. Moreover, while the presented API includes data structures and algorithm steps pertinent to multi-dimensional CFD grid coupling, presented examples featured zero-dimensional setups, for brevity. In PySDM, the backend API is extended to handle general form of coalescence kernels, representation of particle displacement and condensational growth of particles, and the examples shipped with the package include multi-dimensional simulations. SDM algorithm is applicable in other domains of computational modelling, and the scope of the presented material covered the aspects **relevant for coagulation modelling for a wide range of phenomena**.

Acknowledgements

We thank Shin-ichiro Shima and Michael Olesik for helpful discussions. Thanks are due to Numba and ThrustRTC developers for responding to our questions, bug reports and feature requests posted during development of PySDM.

References

1. Andrejczuk, M., Grabowski, W.W., Reisner, J., Gadian, A.: Cloud-aerosol interactions for boundary layer stratocumulus in the lagrangian cloud model. *J. Geophys. Res. Atmos.* (2010), <https://doi.org/10.1029/2010JD014248>
2. Arabas, S., Jaruga, A., Pawlowska, H., Grabowski, W.W.: libcloudph++ 1.0: a single-moment bulk, double-moment bulk, and particle-based warm-rain microphysics library in C++. *Geosci. Model Dev.* (2015), <https://doi.org/10.5194/gmd-8-1677-2015>
3. Arabas, S., Shima, S.: Large-eddy simulations of trade wind cumuli using particle-based microphysics with monte carlo coalescence. *J. Atmos. Sci.* (2013), <https://doi.org/10.1175/JAS-D-12-0295.1>
4. Bacher, A., Bodini, O., Hollender, A., Lumbroso, J.: Mergeshuffle: A very fast, parallel random permutation algorithm (2005), <https://arXiv.org/abs/1508.03167>
5. Bartman, P., et al.: (2021), <https://github.org/atmos-cloud-sim-uj/PySDM>
6. Berry, E.: Cloud droplet growth by collection. *J. Atmos. Sci.* (1966), [https://doi.org/10.1029/1520-0469\(1967\)024\(0688:CDGBC\)2.0.CO;2](https://doi.org/10.1029/1520-0469(1967)024(0688:CDGBC)2.0.CO;2)
7. Chandrasekhar, S.: Stochastic problems in physics and astronomy. *Rev. Mod. Phys.* (1943), <https://doi.org/10.1103/RevModPhys.15.1>

8. DeVile, R.E., Riemer, N., West, M.: Weighted Flow Algorithms (WFA) for stochastic particle coagulation. *J. Comput. Phys.* (2011), <https://doi.org/10.1016/j.jcp.2011.07.027>
9. Dziekan, P., Pawlowska, H.: Stochastic coalescence in Lagrangian cloud microphysics. *Atmos. Chem. Phys.* (2017), <https://doi.org/10.5194/acp-17-13509-2017>
10. Dziekan, P., Waruszewski, M., Pawlowska, H.: University of Warsaw Lagrangian Cloud Model (UWLCM) 1.0: a modern large-eddy simulation tool for warm cloud modeling with Lagrangian microphysics. *Geosc. Model Dev.* (2019), <https://doi.org/10.5194/gmd-12-2587-2019>
11. Gillespie, D.: The stochastic coalescence model for cloud droplet growth. *J. Atmos. Sci.* (1972), [https://doi.org/10.1175/1520-0469\(1972\)029%3C1496:TSCMFC%3E2.0.CO;2](https://doi.org/10.1175/1520-0469(1972)029%3C1496:TSCMFC%3E2.0.CO;2)
12. Golovin, A.: The solution of the coagulation equation for raindrops. Taking condensation into account. *Bull. Acad. Sci. SSSR Geophys. Ser.* (1963), <http://mi.mathnet.ru/dan27630>, in Russian
13. Grabowski, W., Morrison, H., Shima, S., Abade, G., Dziekan, P., Pawlowska, H.: Modeling of cloud microphysics: Can we do better? *Bull. Am. Meteorol. Soc.* (2019), <https://doi.org/10.1175/BAMS-D-18-0005.1>
14. Hansen, K.: Abundance distributions; large scale features. In: *Statistical Physics of Nanoparticles in the Gas Phase*. Springer, Cham (2018), http://doi.org/10.1007/978-3-319-90062-9_8
15. Jensen, J.B., Lee, S.: Giant sea-salt aerosols and warm rain formation in marine stratocumulus. *J. Atmos. Sci.* (2008), <https://doi.org/10.1175/2008JAS2617.1>
16. Lam, S., Pitrou, A., Seibert, S.: Numba: a LLVM-based Python JIT compiler. In: *Proceedings of the Second Workshop on the LLVM Compiler Infrastructure in HPC. LLVM '15*, ACM (2015). <https://doi.org/10.1145/2833157.2833162>
17. Li, X.Y., Brandenburg, A., Haugen, N.E., Svensson, G.: Eulerian and Lagrangian approaches to multidimensional condensation and collection. *J. Adv. Model. Earth Sy.* (2017), <https://doi.org/10.1002/2017MS000930>
18. Shima, S., Kusano, K., Kawano, A., Sugiyama, T., Kawahara, S.: The super-droplet method for the numerical simulation of clouds and precipitation: a particle-based and probabilistic microphysics model coupled with a non-hydrostatic model. *Q. J. Royal Meteorol. Soc.* (2009), <https://doi.org/10.1002/qj.441>
19. Shima, S., Sato, Y., Hashimoto, A., Misumi, R.: Predicting the morphology of ice particles in deep convection using the super-droplet method: development and evaluation of SCALE-SDM 0.2.5-2.2.0, -2.2.1, and -2.2.2. *Geosci. Model Dev.* (2020), <https://doi.org/10.5194/gmd-13-4107-2020>
20. Shima, S., Sugiyama, T., Kusano, K., Kawano, A., Hirose, S.: Simulation method, simulation program, and simulator (2007), <https://data.epo.org/gpi/EP1847939A3>
21. Smoluchowski, M.: Drei vorträge über diffusion, brownsche molekularbewegung und koagulation von kolloidteilchen i. *Phys. Z.* (1916), <https://jbc.bj.uj.edu.pl/dlibra/publication/411755/edition/387533/content>
22. Smoluchowski, M.: Drei vorträge über diffusion, brownsche molekularbewegung und koagulation von kolloidteilchen ii. *Phys. Z.* (1916), <https://jbc.bj.uj.edu.pl/dlibra/publication/411756/edition/387534/content>
23. Unterstrasser, S., Hoffmann, F., Lerch, M.: Collisional growth in a particle-based cloud microphysical model: insights from column model simulations using LCM1D (v1.0). *Geosci. Model Devel.* (2020), <https://doi.org/10.5194/gmd-13-5119-2020>
24. Yang, F.: CURandRTC (Jan 2021), <https://github.com/fynv/CURandRTC>
25. Yang, F.: ThrustRTC (Jan 2021), <https://github.com/fynv/ThrustRTC>